

THE SENSITIVITY OF THE INPUT IMPEDANCE PARAMETERS OF TRACK CIRCUITS TO CHANGES IN THE PARAMETERS OF THE TRACK

Lubomir IVANEK¹, Vladimir MOSTYN², Karel SCHEE³, Jan GRUN³

¹Department of Electrical Engineering, Faculty of Electrical Engineering and Computer Science, VSB–Technical University of Ostrava, 17. listopadu 15, 708 00 Ostrava-Poruba, Czech Republic

²Department of Robotics, Faculty of Mechanical Engineering, VSB–Technical University of Ostrava, 17. listopadu 15, 708 00 Ostrava-Poruba, Czech Republic

³Prvni signalni a.s., Bohuminska 368/172, 712 00 Ostrava-Muglinov, Czech Republic

lubomir.ivanek@vsb.cz, vladimir.mostyn@vsb.cz, schee@1sig.cz, grun@1sig.cz

DOI: 10.15598/aeee.v15i1.1996

Abstract. *This paper deals with the sensitivity of the input impedance of an open track circuit in the event that the parameters of the track are changed. Weather conditions and the state of pollution are the most common reasons for parameter changes. The results were obtained from the measured values of the parameters R (resistance), G (conductance), L (inductance), and C (capacitance) of a rail superstructure depending on the frequency. Measurements were performed on a railway siding in Orlova. The results are used to design a predictor of occupancy of a track section. In particular, we were interested in the frequencies of 75 and 275 Hz for this purpose. Many parameter values of track substructures have already been solved in different works in literature. At first, we had planned to use the parameter values from these sources when we designed the predictor. Deviations between them, however, are large and often differ by three orders of magnitude (see Tab. 8). From this perspective, this article presents data that have been updated using modern measurement devices and computer technology. And above all, it shows a transmission (cascade) matrix used to determine the parameters.*

1. Introduction

In this article, the results of measuring the parameters of rail traction - the resistance of the track circuit, the conductance between the rails, and the inductance and the capacitance of the track circuit - are described. The sensitivity of the input impedance of the track circuit is calculated after changing the parameters of the track. These parameters were investigated to design the predictor, which detects the occupancy of the rail traction. This article does not provide a new method of measurement. The modified Ohm impedance measurement method was used in the measurement. However, elaboration of the results must provide parameter values in a form which can be directly used in a laboratory simulation of track circuits. This simulator was assembled from type two-ports (parameters G , R , L , C) and it was used to verify the device characteristics to predict the occupancy of the track circuit. Thus, cascade coefficients were used for evaluating traction parameters, as well as for elaboration of the measured values in the simulator. Therefore, it is possible to immediately correct potential deficiencies of the simulator.

All these parameters were calculated as specific parameters, which means they were recalculated to the unit length (km) of the tracks.

The following approach was chosen to determine the primary parameters:

- Measurement of the input impedance of an open circuit and input impedance of a section of a railway line terminated with a short circuit.
- Calculation of cascade coefficients.

Keywords

Impedance, parameter estimation, railway safety, sensitivity analysis.

- Calculation of impedance and admittance of two-ports of type II, T and Γ .
- Calculation of the primary two-port parameters and their conversion to the unit length.

Measurements were performed in the Orlova locality in the rail yard of a private firm, AWT. The section of the measured track did not have any track crossings or track branches and had only a slight radius of curvature of the track. The railway yard was very dirty from coal dust, loam and clay, dry fallen leaves, twigs, and so on. The weather was rainy. It was raining slightly when the measurements were taken, and had been raining for a long time beforehand. The length of the track section was 540 m.

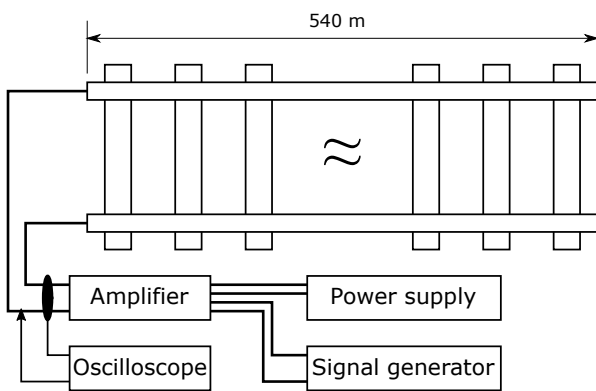


Fig. 1: Connection diagram.

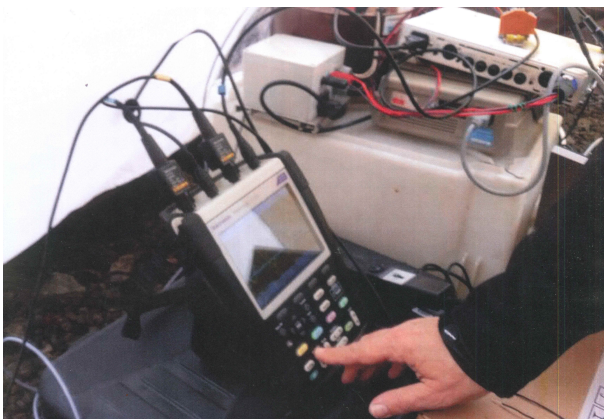


Fig. 2: View of the workplace arrangement.

Examples of display of the measured waveforms on the oscilloscope:

At lower frequencies, the current leads the voltage on empty track (see Fig. 3).

The voltage leads the current at higher frequencies and therefore the track circuit has an inductive character. Figure 4 shows an example of waveforms for a track

that was shunted to 524 m away from the measuring site.

The track circuit in Fig. 4 certainly has an inductive character.

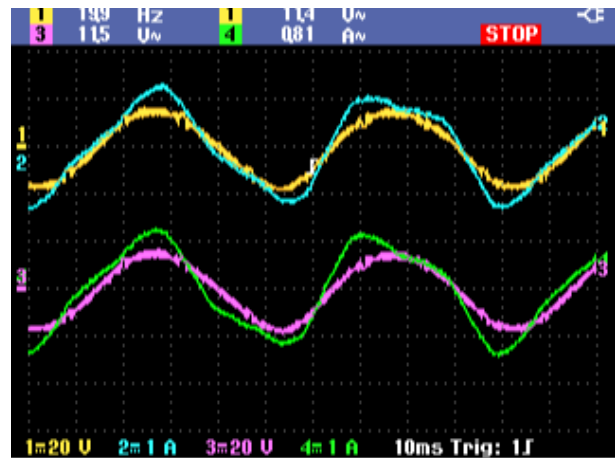


Fig. 3: Voltage and current courses for the frequency of 19.9 Hz.

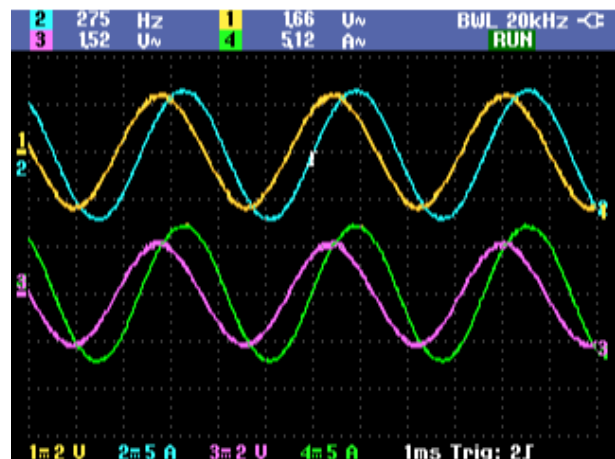


Fig. 4: Voltage and current waveforms for the frequency of 275 Hz.

A device for prediction of occupancy of the track circuit must be regularly calibrated during operation when weather conditions are changing. Calibration will be done on unoccupied track circuits. In an open circuit of the traction, mostly capacity and conductivity of the substructures may be varied. Therefore, we are

Tab. 1: Assignment of oscilloscope channels to the measured quantities.

| No. | Quantity | Function |
|-----|----------|---|
| CH1 | U1 | Voltage at the amplifier output |
| CH2 | I1 | The output current from an amplifier |
| CH3 | U2 | Voltage between the rails at the measuring location |
| CH4 | I2 | Current to rails |

Tab. 2: Module and phase of impedance of open traction circuit and short traction circuit.

| Impedance open circuit | | | Impedance short circuit | | |
|---------------------------|------------------------|-------------------------|---------------------------|------------------------|-------------------------|
| f _{524m} (Hz) | Z _{op} (Ω) | ϕ _o (rad) | f _{524m} (Hz) | Z _{sh} (Ω) | ϕ _s (rad) |
| 19.89 | 14.47 | -0.26 | 19.43 | 0.44 | 0.36 |
| 50.26 | 13.44 | -0.14 | 49.74 | 0.67 | 0.76 |
| 74.76 | 13.25 | -0.1 | 75.86 | 0.85 | 0.83 |
| 100.51 | 13.8 | -0.09 | 100.23 | 1.1 | 0.89 |
| 123.57 | 12.99 | -0.06 | 125.32 | 1.18 | 0.93 |
| 149.86 | 12.94 | -0.09 | 150.59 | 1.34 | 0.99 |
| 173.21 | 12.84 | -0.06 | 174.85 | 1.49 | 0.99 |
| 202.7 | 12.72 | -0.07 | 199.82 | 1.64 | 1.1 |
| 250.73 | 12.66 | -0.08 | 248.55 | 1.9 | 1.4 |
| 274.19 | 12.62 | -0.05 | 275.29 | 2.4 | 1.8 |
| 302.48 | 12.27 | -0.01 | 303.74 | 2.2 | 1.6 |
| 491.28 | 11.93 | 0.05 | 500.87 | 3.24 | 1.11 |
| 1009.77 | 11.93 | 0.13 | 1032.62 | 5.81 | 1.17 |

interested in finding out how the parameters change as the weather changes, and which parameter of the device will be the most responsive one. This parameter will be determining during the calibration of the instrument.

2. Open and Short Circuit Impedance

Measurements were performed for the frequency range from 20 to 5000 Hz. The length of the measured section of rail traction was 540 m. The courses were obtained in the form of graphs (Fig. 3 and Fig. 4) and in table form. The obtained curves expressed in tabular form contained a large amount of noise and in order to use them, they had to be approximated by a sine wave function - (Fig. 5).

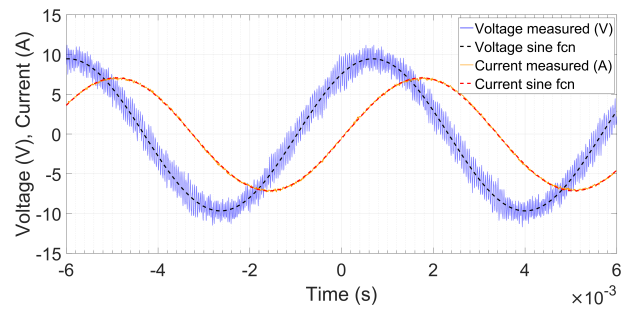
The measured values were the magnitude Z and the phase φ of the input impedance at the beginning of the track circuits. Measurements were performed under the open circuit Z_{op} and short circuit Z_{sh} . It is clear from Tab. 2 that the frequency at which the impedances are measured in the open and short circuits are not completely identical. Therefore, three kinds of interpolation by polynomials were performed for both curves: cubic spline interpolation, B-spline interpolation, and polynomial regression.

$$\begin{aligned} vsc &:= cspline(vx, vy), \\ vsb &:= bspline(vx, vy, u, 2), \\ vsr &:= regress(vx, vy, 3). \end{aligned} \quad (1)$$

From these polynomials, impedance values have been assigned to the same integer frequencies (see Tab. 3).

Impedance components were converted to the form of complex numbers using a simple Eq. (2):

$$\underline{Z} = Ze^{j\varphi} = Z(\cos\varphi + j\sin\varphi). \quad (2)$$

**Fig. 5:** Example of interleaving of the actual course of state variables by the sine function.**Tab. 3:** Impedance of the open circuit and the short circuit.

| Freq. | Z _{op} (Ω) | Z _{sh} (Ω) |
|-------|---------------------|---------------------|
| 20 | 13.99-3.73j | 0.42+0.16j |
| 50 | 13.3-1.95j | 0.48+0.46j |
| 75 | 13.18-1.4j | 0.57+0.64j |
| 100 | 13.02-1.28j | 0.63+0.79j |
| 125 | 12.98-0.8j | 0.7+0.96j |
| 150 | 12.89-1.2j | 0.73+1.13j |
| 175 | 12.82-0.87j | 0.82+1.25j |
| 200 | 12.7-0.9j | 0.87+1.4j |
| 250 | 12.61-1.09j | 0.95+1.65j |
| 275 | 12.54-0.39j | 0.96+1.81j |
| 300 | 12.27-0.15j | 1.07+1.93j |
| 500 | 11.91+0.7j | 1.43+2.91j |
| 1000 | 11.83+1.61j | 2.25+5.36j |
| 3000 | 12.01+0.46j | 6.8+11.54j |
| 5000 | 11.99+7.79j | 11.31+14.38j |

3. Calculation of the Cascade Coefficients

Matrix of cascade coefficients:

$$\underline{A} = \begin{vmatrix} \sqrt{\frac{Z_{op}}{Z_{op}-Z_{sh}}} & Z_{sh} \sqrt{\frac{Z_{op}}{Z_{op}-Z_{1k}}} \\ \frac{1}{\sqrt{Z_{op}(Z_{op}-Z_{sh})}} & \sqrt{\frac{Z_{op}}{Z_{op}-Z_{sh}}} \end{vmatrix}. \quad (3)$$

Primarily we are interested in the frequency of 75 Hz with the wavelength of 1154701 m, and secondarily, the frequency of 275 Hz with the wavelength of 314918.3 m. Consequently, the 524 m segment of the railway can be considered as an elementary line section - for example as a two-port of type T or II with a matrix of cascade coefficients according to Tab. 4.

Coefficient A_{12} was negative for frequencies above 1000 Hz. Also, the determinant of the matrix coefficients from this frequency was not equal to zero. Therefore, these values were not used again. The frequencies of 75 and 275 Hz interest us most.

Cascade coefficients were also calculated from the secondary circuit parameters:

$$\underline{Z}_0 = \sqrt{\underline{Z}_{10} \underline{Z}_{1k}}, \quad (4)$$

$$\tanh(\underline{g}_0) = \sqrt{\frac{\underline{Z}_{1k}}{\underline{Z}_{10}}} \Rightarrow \underline{g}_0 = \frac{1}{2} \ln \left(\frac{1 + \sqrt{\frac{\underline{Z}_{1k}}{\underline{Z}_{10}}}}{1 - \sqrt{\frac{\underline{Z}_{1k}}{\underline{Z}_{10}}}} \right). \quad (5)$$

From these secondary parameters, the following equation is valid:

$$\underline{A}_{22} = \underline{A}_{11} = \frac{e^{\underline{g}_0} + e^{-\underline{g}_0}}{2} = \cosh(\underline{g}_0), \quad (6)$$

$$\underline{A}_{12} = \underline{Z}_0 \sinh(\underline{g}_0). \quad (7)$$

Tab. 4: Cascade coefficients.

| Freq. | \underline{A}_{11} | \underline{A}_{12} | \underline{A}_{21} |
|-------|----------------------|----------------------|----------------------|
| 20 | 1.013+0.009j | 0.424+0.166j | 0.067+0.019j |
| 50 | 1.014+0.020j | 0.478+0.477j | 0.074+0.012j |
| 75 | 1.018+0.028j | 0.563+0.667j | 0.076+0.010j |
| 100 | 1.020+0.034j | 0.615+0.827j | 0.077+0.010j |
| 125 | 1.020+0.041j | 0.676+1.011j | 0.078+0.008j |
| 150 | 1.021+0.049j | 0.690+1.190j | 0.078+0.011j |
| 175 | 1.025+0.055j | 0.772+1.327j | 0.079+0.010j |
| 200 | 1.026+0.062j | 0.805+1.490j | 0.080+0.011j |
| 250 | 1.025+0.074j | 0.851+1.762j | 0.080+0.013j |
| 275 | 1.028+0.081j | 0.841+1.939j | 0.082+0.009j |
| 300 | 1.034+0.089j | 0.935+2.091j | 0.084+0.008j |
| 500 | 1.046+0.140j | 1.088+3.245j | 0.088+0.007j |
| 1000 | 1.043+0.271j | 0.894+6.198j | 0.089+0.011j |
| 3000 | 0.826+0.547j | -0.694+13.252j | 0.070+0.043j |
| 5000 | 0.766+1.253j | -9.357+25.195j | 0.093+0.044j |

4. Calculation of Parameters of Two-port

The measured part of traction was replaced by a two-port of type II. This two-port can be described as a matrix Eq. (8):

$$\underline{A} = \begin{bmatrix} 1 + \underline{Y}\underline{Z} & \underline{Z} \\ \underline{Y}\underline{Z} + \underline{Y}^2\underline{Z} & 1 + \underline{Y}\underline{Z} \end{bmatrix}. \quad (8)$$

Thus

$$\underline{Z} = \underline{A}_{12}, \quad (9)$$

$$\underline{Y} = \frac{\underline{A}_{11} - 1}{\underline{Z}}. \quad (10)$$

From the matrix Eq. (8), we have calculated the parameters of the two-port (see Tab. 5 and Tab. 6). The parameter values R, G, L, and C were converted to a unit length of 1 km.

Tab. 5: Parameters of two-port.

| Freq. | $\underline{Z}(\Omega)$ | $\underline{Y}(S)$ |
|-------|-------------------------|--------------------|
| 20 | 0.453+0.149j | 0.032+0.016j |
| 50 | 0.575+0.493j | 0.037+0.004j |
| 75 | 0.565+0.665j | 0.038+0.003j |
| 100 | 0.653+0.812j | 0.038+0.005j |
| 125 | 0.660+1.014j | 0.039+0.001j |
| 150 | 0.721+1.188j | 0.039+0.001j |
| 175 | 0.841+1.286j | 0.038+0.010j |
| 200 | 0.798+1.519j | 0.040+0.001j |
| 250 | 0.897+1.763j | 0.039+0.007j |
| 275 | 0.860+1.941j | 0.040+0.001j |
| 300 | 0.926+2.114j | 0.040+0.002j |
| 500 | 1.079+3.233j | 0.041+0.003j |
| 1000 | 0.839+6.020j | 0.043+0.004j |

Tab. 6: The resulting values for the parameters R, G, L, and C of the type II two-port.

| Freq. | $\underline{R} \cdot \text{km}^{-1}$ | $\underline{G} \cdot \text{km}^{-1}$ | $\underline{L} \cdot \text{km}^{-1}$ | $\underline{C} \cdot \text{km}^{-1}$ |
|-------|--------------------------------------|--------------------------------------|--------------------------------------|--------------------------------------|
| 20 | 0.839 | 0.118 | 0.0022 | 0.000458 |
| 50 | 1.6 | 0.139 | 0.0029 | 0.0000468 |
| 75 | 1.5 | 0.141 | 0.00261 | 0.0000258 |
| 100 | 1.21 | 0.142 | 0.00239 | 0.0000304 |
| 125 | 1.22 | 0.144 | 0.00239 | 0.00000352 |
| 150 | 1.34 | 0.145 | 0.00234 | 0.00000348 |
| 175 | 1.56 | 0.14 | 0.00217 | 0.0000361 |
| 200 | 1.48 | 0.147 | 0.00224 | 0.00000342 |
| 250 | 1.66 | 0.146 | 0.00209 | 0.0000158 |
| 275 | 1.59 | 0.149 | 0.00206 | 0.00000324 |
| 300 | 1.72 | 0.15 | 0.00208 | 0.00000328 |
| 500 | 2.00 | 0.154 | 0.0019 | 0.00000315 |
| 1000 | 1.55 | 0.158 | 0.00176 | 0.00000212 |

Tab. 7: The resulting values for the parameters R, G, L, and C converted to a unit length of 1 km.

| Freq. | $\underline{R} \cdot \text{km}^{-1}$ | $\underline{G} \cdot \text{km}^{-1}$ | $\underline{L} \cdot \text{km}^{-1}$ | $\underline{C} \cdot \text{km}^{-1}$ |
|-------|--------------------------------------|--------------------------------------|--------------------------------------|--------------------------------------|
| 20 | 0.839 | 0.117 | 0.0022 | $3.08 \cdot 10^{-4}$ |
| 50 | 1.6 | 0.12 | 0.0029 | $9.03 \cdot 10^{-5}$ |
| 75 | 1.5 | 0.14 | 0.00261 | $3.68 \cdot 10^{-5}$ |
| 100 | 1.21 | 0.14 | 0.00239 | $3.43 \cdot 10^{-5}$ |
| 125 | 1.22 | 0.144 | 0.00239 | $1.27 \cdot 10^{-5}$ |
| 150 | 1.34 | 0.142 | 0.00234 | $2.07 \cdot 10^{-5}$ |
| 175 | 1.56 | 0.144 | 0.00217 | $1.94 \cdot 10^{-5}$ |
| 200 | 1.48 | 0.145 | 0.00224 | $1.03 \cdot 10^{-5}$ |
| 250 | 1.69 | 0.144 | 0.00209 | $1.35 \cdot 10^{-5}$ |
| 275 | 1.56 | 0.151 | 0.00206 | $6.46 \cdot 10^{-6}$ |
| 300 | 1.72 | 0.153 | 0.00208 | $3.83 \cdot 10^{-6}$ |
| 500 | 2.2 | 0.16 | 0.0019 | $3.58 \cdot 10^{-7}$ |
| 1000 | 1.62 | 0.169 | 0.00176 | $-2.63 \cdot 10^{-7}$ |

Graphs of the dependence of these parameters on the frequency are shown in Fig. 6, Fig. 7, Fig. 8 and Fig. 9.

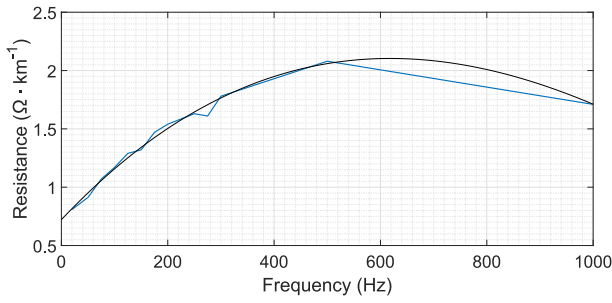


Fig. 6: Specific resistance as a function of frequency.

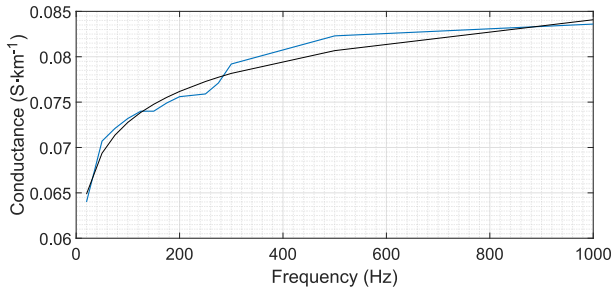


Fig. 7: Specific conductance as a function of frequency.

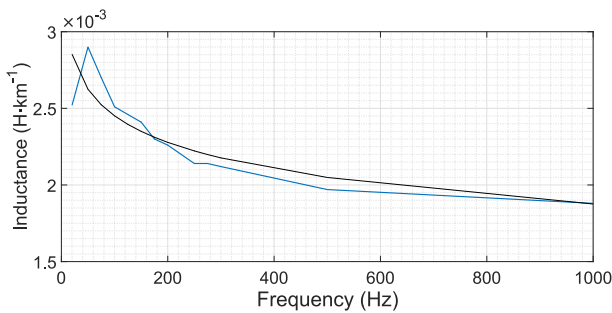


Fig. 8: Specific inductance as a function of frequency.

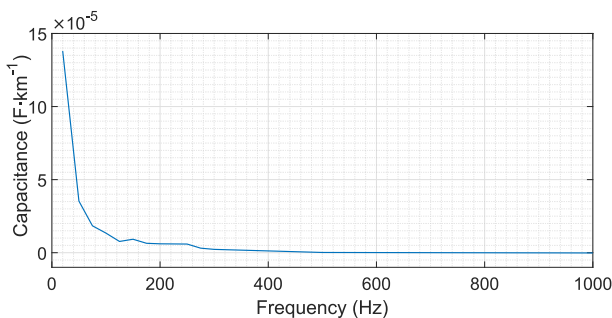


Fig. 9: Specific capacitance as a function of frequency.

5. Calculation of the Sensitivity of the Input Impedance to Changes of Parameters

The parameters of traction circuits change with the weather. First, we determined the sensitivity of the

input impedance of the open circuit when changing the individual parameters. Thus we found which parameter affected the function of the predictor predominantly, and vice versa, which one can possibly be neglected. The assessed frequency was 275 Hz. Thus, we used these values:

Tab. 8: Used values of R, G, L and C.

| $R \cdot \text{km}^{-1}$ | $G \cdot \text{km}^{-1}$ | $L \cdot \text{km}^{-1}$ | $C \cdot \text{km}^{-1}$ |
|--------------------------|--------------------------|--------------------------|--------------------------|
| 1.56 | $1.51 \cdot 10^{-1}$ | $2.06 \cdot 10^{-3}$ | $6.46 \cdot 10^{-6}$ |

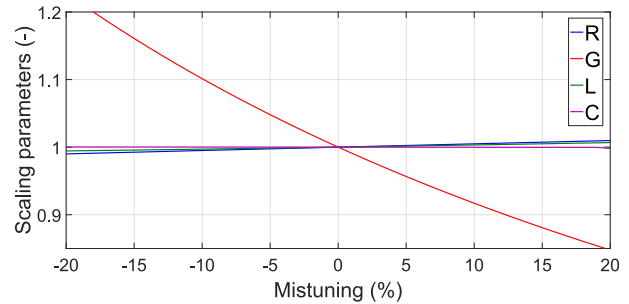


Fig. 10: Dependence of changes of normed real component of impedance in the open circuit on the percentage change of each parameter.

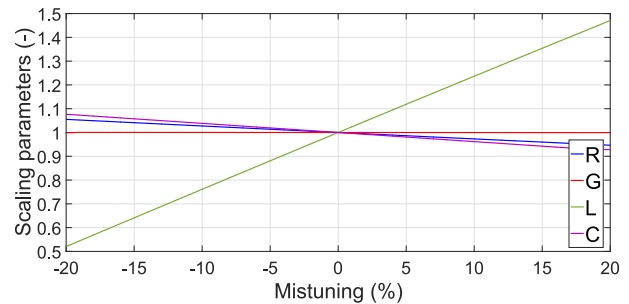


Fig. 11: Dependence of changes of the normed imaginary component of impedance in the open circuit on the percentage change of each parameter.

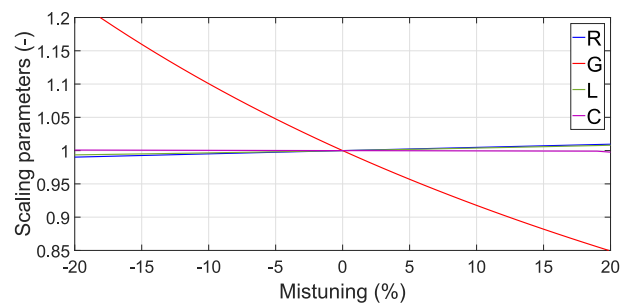


Fig. 12: Dependence of changes of normed magnitude of impedance in the open circuit on the percentage change of each parameter.

These parameters were gradually mistuning about 20 % in both the positive and the negative values while the values of the other parameters remained constant.

6. Conclusion

The measurements that are described herein are intended for the design of a predictor that searches the occupancy of the track circuit. This predictor needs to react to weather changes and changes of other conditions of traction. Therefore, repeated measurements must be carried out, especially in the open circuit condition. When measuring under open circuit conditions, it is necessary to evaluate the particular ratio of effective values of voltages and currents and thus to evaluate the magnitude of the impedance. It is most sensitive to changes of conductance G . Conductance G and capacitance C change the most with the weather conditions. Thus is enough, if only the change of the conductivity G is respected during calibration. Other parameters remain constant.

Finally, we compared the calculated values with those from various works in literature for the frequency of 275 Hz.

Tab. 9: Comparison of our results with those of other papers.

| $R \cdot \text{km}^{-1}$ (Ω) | $G \cdot \text{km}^{-1}$ (S) | $L \cdot \text{km}^{-1}$ (H) | $C \cdot \text{km}^{-1}$ (F) | Ref. |
|--|---------------------------------|---------------------------------|---------------------------------|------|
| 0.55 | 2.25 | $1.55 \cdot 10^{-3}$ | $0.25 \cdot 10^{-6}$ | [2] |
| 1.1 | $1.04 \cdot 10^{-3}$ | - | $0.9 \cdot 10^{-6}$ | [4] |
| 0.18 | $18 \cdot 10^{-3}$ | $12.7 \cdot 10^{-3}$ | $7 \cdot 10^{-6}$ | [5] |
| 0.004 | - | $1.45 \cdot 10^{-3}$ | - | [8] |
| 1.56 | $1.51 \cdot 10^{-1}$ | $2.06 \cdot 10^{-3}$ | $6.46 \cdot 10^{-6}$ | [*] |

[*] this paper

However, it is too difficult to compare the values of measurements under different conditions at different shunt resistances conducted in series to the rails when measuring the short circuit and so on. The measuring conditions are not comparable at all.

Acknowledgment

This research is supported by the project SP 2016/143 "Research of antenna systems; effectiveness and diagnostics of electric drives with harmonic power; reliability of the supply of electric traction; issue data anomalies." and by the project TA04031780 "AXIO - a system for measuring distance and speed of rail vehicles.

References

- [1] MARISCOTTI, A. and P. POZZOBON. Determination of the electrical parameters of railway traction lines: calculation, measurement, and reference data. *IEEE Transactions on Power Delivery*. 2004, vol. 19, no. 4, pp. 1538–1546. ISSN 0885-8977. DOI: 10.1109/TPWRD.2004.835285.
- [2] COLAK, K. and M. H. HOCAOGLU. Calculation of rail potentials in a DC electrified railway system. In: *38th International Universities Power Engineering Conference*. Thessaloniki: UPEC, 2003, pp. 5–8.
- [3] HILL, R. J., S. BRILLANTE and P. J. LEONARD. Railway track transmission line parameters from finite element field modelling: Series impedance. *IEEE Proceeding Electric Power Applications*. 1999, vol. 146, iss. 6, pp. 647–660. ISSN 1350-2352. DOI: 10.1049/ip-epa:19990649.
- [4] HILL, R. J. and D. C. CARPENTER. Rail track distributed transmission line impedance and admittance: theoretical modeling and experimental results. *IEEE Transaction Vehicular Technology*. 1993, vol. 42, iss. 2, pp. 225–241. ISSN 0018-9545. DOI: 10.1109/25.211460.
- [5] HILL, R. J., D. C. CARPENTER and T. TASAR. Railway track admittance, earth-leakage effects and track circuit operation. In: *Technical Papers Presented at the 1989 IEEE/ASME Joint Railroad Conference*. Philadelphia: IEEE, 1989, pp. 55–62. ISBN 0-7803-3854-5. DOI: 10.1109/RRCON.1989.77281.
- [6] GARG, R., P. MAHAJAN and P. KUMAR. Sensitivity Analysis of Characteristic Parameters of Railway Electric Traction System. *International Journal of Electronics and Electrical Engineering*. 2014, vol. 2, no. 1, pp. 8–14. ISSN 2301-380X. DOI: 10.12720/ijeee.2.1.8-14.
- [7] SZELAG, A. Rail track as a lossy transmission line Part I: Parameters and new measurement methods. *Archives of Electrical Engineering*. 2000, vol. XLIX, no. 3–4, pp. 407–423. ISSN 1427-4221.
- [8] HOLMSTROM, F. R. The model of conductive interference in rapid transit signaling systems. *IEEE Transactions on Industry Applications*. 1986, vol. IA-22, iss. 4, pp. 756–762. ISSN 0093-9994. DOI: 10.1109/TIA.1986.4504788.
- [9] SZELAG, A. Rail track as a lossy transmission line. Part II: New method of measurements-simulation and in situ measurements. *Archives of Electrical Engineering*. 2000, vol. XLIX, no. 3–4, pp. 425–453. ISSN 1427-4221.
- [10] JOURNEY, M. P., O. J. STEEL and B. K. FORTE. Electromagnetic modeling of electric railway systems to study its compatibility. *Revista Digital Lampsakos*. 2010, vol. 2010, no. 3, pp. 42–47, ISSN 2145-4086. DOI: 10.21501/issn.2145-4086.

- [11] GUGLIELMINO, E. Determinacion de parametros electromagneticos de vias ferreas. *Ingenierias*. 2003, vol. VI, no. 19, pp. 39–46. ISSN 1405-7743.
- [12] NOLAN, D., P. MCGREGOR and J. PAFF. TMG E1631 - Westinghouse FS2600 Track Circuits Manual. *Transport for NSW* [online]. 2015. Available at: <http://www.asa.transport.nsw.gov.au/sites/default/files/asa/railcorp-legacy/disciplines/signals/tmg-e1631.pdf>.
- [13] HUAN, Q., Y. ZHANG. and B. ZHAO. Study on shunt state of track circuit based on transient current. *WSEAS Transactions on Circuits and Systems*. 2015, vol. 14, iss. 1, pp. 1–7. ISSN 2224-266X.
- [14] GARCIA, J. C., J. A. JIMENEZ, F. ESPINOSA, A. HERNANDEZ, I. FERNANDEZ, M. C. PEREZ, J. URENA, M. MAZO and J. J. GARCIA. Characterization of railway line impedance based only on short-circuit measurements. *International Journal of Circuit Theory and Applications*. 2015, vol. 43, no. 8, pp. 984–994. ISSN 1097-007X. DOI: 10.1002/cta.1987.

About Authors

Lubomir IVANEK was born in Frydek Mistek in the Czech Republic. He graduated from the VSB–Technical University Ostrava, Faculty of Mechanical and Electrical Engineering, earned his Ph.D. degree from the Czech Technical University in Prague, Department of Theoretical Electrical Engineering. He received his Associate Professor degree at the

VSB–Technical University of Ostrava in the field of Theoretical Electrical Engineering. His research involves the waves propagation and antennas, mathematical modelling of the electromagnetic field, stray current under electric tractions.

Vladimir MOSTYN was born in Prilepy in the Czech Republic. He received the M.Sc. degree in Electrical Engineering in 1979 from the VSB–Technical University of Ostrava, Czech Republic. Since 1990, he has been an Assistant Professor with the Department of Robotics and he received the Ph.D. degree in 1996 in Control Engineering at the same university. In 2006, after successful accomplishment of the professorship at the Technical University of Kosice, he was appointed Professor in the branch of Production Systems with Industrial Robots and Manipulators, by the president of the Slovak Republic. Now he is working as a professor at the Department of Robotics at the Faculty of Mechanical Engineering at the VSB–Technical University of Ostrava, Czech Republic. He is the author of two books and more than 80 articles. Prof. V. Mostyn is an Associate Editor of the journal *MM Science Journal* and the member of Czech Association of Robotic Surgery.

Karel SCHEE was born in Opava, Czech Republic. He received his M.Sc. from VSB–Technical University Ostrava in 1999. His research interests include automation of rail transport.

Jan GRUN was born in Ostrava, Czech Republic. He received his M.Sc. from Kiev Technical University (KPI) in 1985. He is engaged in design automation HW rail transport.